# A Compact Model of FDSOI based 1-T Pixel Sensor for Design of In-sensor Computing

G. H. Yu, Z. Zhou*, R. Q. Chen, J. Q. Li, Y. Xiao, P. Huang, J. F. Kang, X. Y. Liu#
School of Integrated Circuits, Peking University, Beijing, 100871, China.
Beijing Advanced Innovation Center for Integrated Circuits, Beijing 100871, China
Email: zhouzime@pku.edu.cn*, liuxiaoyan@pku.edu.cn#

***Abstract*—A compact model for photoresponse of Fully-Depleted Silicon-on-Insulator (FDSOI) based one-transistor (1-T) pixel sensor is proposed for the design of in-sensor computing. The model describes the photoresponse as the photoelectrons charging the device equivalent capacitors to obtain the threshold voltage ($V_{th}$) change and it is verified by both the TCAD and device in 22nm FDSOI technology node. By integrating the model into BSIM-IMG, the accuracy of array-scale in-sensor Vector-Matrix Multiplication (VMM) affected by device doping variation is evaluated using HSPICE.**

***Keywords—Compact model, 1-T pixel sensor, In-sensor Computing, FDSOI***

## I. Introduction

To reduce redundant data movement for efficient machine vision systems, the in-sensor computing (ISC) paradigm [1, 2] has been proposed recently by integrating parts of post-processing into the sensor. Various process functions have been implemented in the pixel array, such as move detection [3] and VMM operation [4], which significantly improved the overall performance. Benefit from the excellent CMOS compatibility and pixel functions monolithic integration, the novel 1-T pixel sensor based on FDSOI technology [5, 6] is an outstanding candidate for ISC. The compact model of this sensor is vital for the efficient evaluation of the array-scale photoelectric characteristics, as well as for the design in ISC applications. In this work, we propose a compact model for the photoresponse of FDSOI 1-T sensor to obtain its light-induced $V_{th}$ change ($\Delta V_{th}$). It is integrated into the BSIM-IMG [7, 8] to quantify the current characteristic with both optical and electrical bias, by which the array-scale in-sensor VMM performance and the influence of device variation can be evaluated using HSPICE.

## II. Model Description & Verification

As shown in Fig.1(a), the FDSOI based 1-T pixel sensor is composed of a FDSOI MOSFET with p-doped substrate under the buried oxide (BOX). It has four terminals: drain, gate, source on transistor and back bias on substrate. The exposure region is the part without the block of metal lines and gate. As shown in Fig.1(b), Its $I_D$ decreases with exposure after applying negative $V_B$, which is measured from the device fabricated by 22nm FDSOI technology [5, 9]. The photoresponse mechanism is that depletion region under the BOX is pulled out by $V_B$ and the photoelectrons together with dark-electrons are gradually accumulated by it. The potential under the BOX ($\varphi_{BS}$) is consequently decreased and the transistor $V_{th}$ is increased due to back-gate modulation.

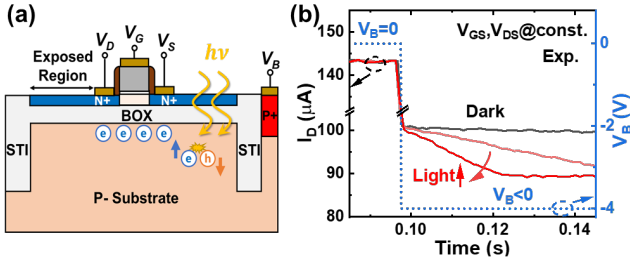


**Fig.1 a)** The schematic of FDSOI based 1-T pixel sensor. The gathered photoelectrons under the BOX cause the back-gate modulation to transistor. **b)** The measured device photoresponse characteristic. After applying negative $V_B$, the $I_D$ decreases and then saturated over time under light exposure.

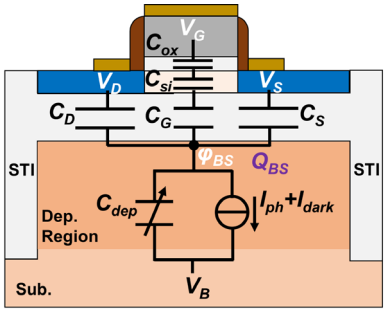


**Fig.2** The photoresponse model description. The response is described as photo-e current ($I_{ph}$) and dark-e current ($I_{dark}$) charging the device equivalent capacitors. There are $Q_{BS}$ electrons accumulated under BOX in the exposure time and $\varphi_{BS}$ is consequently pulled down. The $V_{th}$ of transistor is increased because the $\varphi_{BS}$ acts as the back-gate bias.

As shown in Fig.2, in our model, the photoresponse process is described as the charging process of photoelectrons and dark-electrons to the device equivalent capacitors, which are composed of the serial capacitors in the channel region ($C_{OX}||C_{si}||C_G$), the drain/source BOX capacitors ($C_D$/$C_S$) and the depletion region capacitor ($C_{dep}$). Regarding the depletion region as a half p-n junction with only p-part, the photo-electron current ($I_{ph}$) and the dark-electron current ($I_{dark}$) in our model are calculated by the same solutions of the hypothetical half p-part modified from typical photodiode models [10, 11]. The $I_{ph}$ is written as:

$$I_{ph} = A_{ph} * (J_{dr} + J_{diff}) \tag{1}$$

where $A_{ph}$ is the exposure area of the device. $J_{dr}$/$J_{diff}$ is the drifting/diffusing current density of photoelectron, which are:

$$J_{dr} = q\Phi_{ph}[\exp(-\alpha W_{dep}) - 1] \tag{2}$$

$$J_{diff} = \frac{q\Phi_{ph}\alpha^2 L_n^2}{\alpha^2 L_n^2 - 1}\exp(-\alpha W_{dep}) \tag{3}$$

where $\Phi_{ph}=(1-R)P_{opt}/(h\nu)$, $R$ is the light reflectivity, $P_{opt}$ is the light intensity, $h\nu$ is the photon energy. The $\alpha$ is the light absorption coefficient of Si, $W_{dep}$ is the depletion width and the $L_n$ is the electron diffusion length.

The $I_{dark}$ is composed of three parts similar to the complete photodiode, which is written as:

$$I_{Dark} = A_{tot} * (J_S + J_{SRH} + J_{BBT}) \quad (4)$$

where $A_{tot}$ is the total area of the device. $J_S/J_{SRH}/J_{BBT}$ is the intrinsic/Shockley-Read-Hall/Band-to-Band Tunnel current density [11], which are written as:

$$J_S = \frac{qn_i^2 D_n}{N_A L_n}[\exp(\frac{qV_{AK}}{kT}) - 1] \quad (5)$$

$$J_{SRH} = C_{SRH} F_{TD}[\exp(\frac{qV_{AK}}{2kT}) - 1]\omega_{SRH} W_{dep} \quad (6)$$

$$J_{BBT} = C_{BBT} V_{AK} F_{\max}^2 \exp(\frac{-F_{BBT}}{F_{\max}}) \quad (7)$$

where the $C_{SRH}/C_{BBT}/F_{BBT}$ are the adjustable model parameters and the other parameters are with the same meanings as described in [11]. The $V_{AK}$ is the difference between the applied voltage and the equilibrium voltage across the depletion region. For the hypothetical half p-part in this model, it is written as:

$$V_{AK} = 2\phi_{Fp} - \varphi_{BS} + V_B \quad (8)$$

where the $\phi_{Fp}$ is the flat band voltage of the substrate and $V_B$ is the voltage applied on the substrate.

Furthermore, the accumulated electrons ($Q_{BS}$) in the exposure time ($t_{int}$) are the integration result of the $I_{ph}$ and $I_{dark}$, which is:

$$Q_{BS} = -\int_{t_{\text{int}}} (I_{ph} + I_{dark})dt \quad (9)$$

After that, solved from the voltage distribution relationships between $C_D/(C_{ox}||C_{Si}||C_G)/C_S/C_{dep}$, the $\varphi_{BS}$ affected by the $Q_{BS}$ under the BOX is written as:

$$\varphi_{BS} = \frac{2B - 4AC - 2\sqrt{B^2 - 4ABC}}{4A^2} + V_B \quad (10)$$

where intermediate variable $A$, $B$, $C$ are written as:

$$A = C_D + C_S + (C_G \,||\, C_{Si} \,||\, C_{ox}) \quad (11)$$

$$B = 2q\varepsilon_{si} N_A A_{tot}^2 \quad (12)$$

$$C = Q_{BS} - C_D(V_D - V_B) - C_S(V_S - V_B) - (C_G \,||\, C_{Si} \,||\, C_{ox})(V_G - V_B) \quad (13)$$

where $\varepsilon_{Si}$ is the dielectric constant of Si, $N_A$ is the doping concentration of substrate, $V_D/V_S/V_G$ is the voltage applied on the Drain/Source/Gate terminal. Finally, the $\Delta V_{th}$ is obtained from the change of $\varphi_{BS}$ in the $t_{int}$ ($\Delta\varphi_{BS}$) based on the back-gate bias sensitivity in the typical SOI MOSFET model [7, 8], which is written as:

$$\Delta V_{th} = -\frac{C_G C_{si}}{(C_G + C_{si})C_{ox}} \Delta\varphi_{BS} \quad (14)$$

As shown in Fig.3(a) and (b), the model results show good agreement with the TCAD for the $\Delta\varphi_{BS}$ and $\Delta V_{th}$

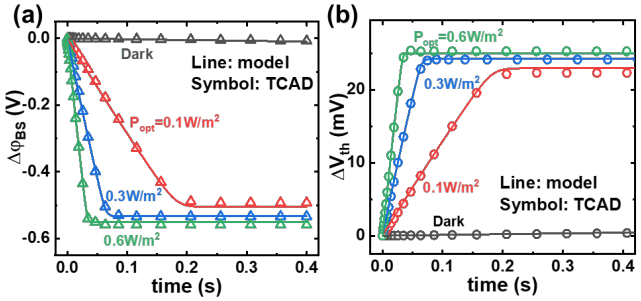


**Fig.3** The evolution of **a)** $\Delta\varphi_{BS}$ and **b)** $\Delta V_{th}$ for device over the time under different incident light intensity ($P_{opt}$). Both these two model results show good agreement with the results from the TCAD.

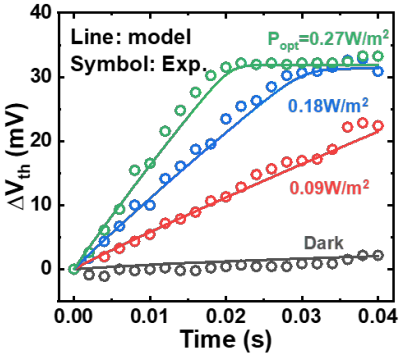


**Fig.4** The $\Delta V_{th}$ under different $P_{opt}$ obtained by the model agrees well with the experiment.

**Tab.1** The adjustable model parameters for measured device. Their roles in the model are also listed.

| Parameter | Role in | Value |
|---|---|---|
| R | $I_{ph}$ | 0.25 |
| $N_A$ | $\Delta\varphi_{BS}$ | $1.1\times10^{18}cm^{-3}$ |
| $C_{SRH}$ | $I_{dark}$ | $4\times10^{3}A/V^3$ |
| $C_{BBT}$ | $I_{dark}$ | $1\times10^{3}A/V^3$ |
| $F_{BBT}$ | $I_{dark}$ | $3\times10^{9}V/m$ |

evolution by the exposure time. The model also shows good agreement with the measured $\Delta V_{th}$ evolution, as shown in Fig.4. There is no fitting parameter in the model. The adjustable parameters are the $R$ affecting the $I_{ph}$, the $N_A$ determining the effect of the $Q_{BS}$ to the $\Delta\varphi_{BS}$, and the $C_{SRH}/C_{BBT}/F_{BBT}$ affecting the $I_{dark}$. These adjustable parameters used for measured device fabricated by 22nm FDSOI technology are listed in Tab.1.

Moreover, the proposed model can be added into the BSIM-IMG [7, 8], the typical FDSOI MOSFET model, to obtain the $I_D$ affected by light as shown in Fig.5. The BSIM-IMG is composed of its core long-gate current model, $V_{th}$ modification models, transport modification and other models. The proposed model describes the light-induced $V_{th}$ change so it is added as an extra $V_{th}$ model into the BSIM-IMG. The $I_D$ results of the model combined with BSIM-IMG can be obtained from HSPICE. As shown in Fig.6(a), the initial dark-state $I_D$ agrees well with the experiments under different $V_B$. The pixel $I_D$ related to the $P_{opt}$ under different $V_{DS}$ also shows good agreement with the measured data, which verifies our model and enables the array-scale evaluation for the ISC performance of the FDSOI 1-T pixel using HSPICE.

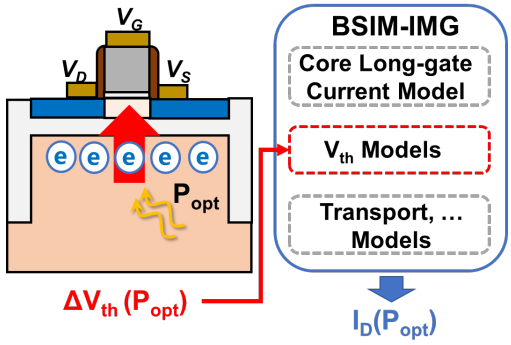


**Fig.5** The light-induced $\Delta V_{th}$ of our model is integrated into the $V_{th}$ models of the BSIM-IMG to obtain the device $I_D$ affected by $P_{opt}$.

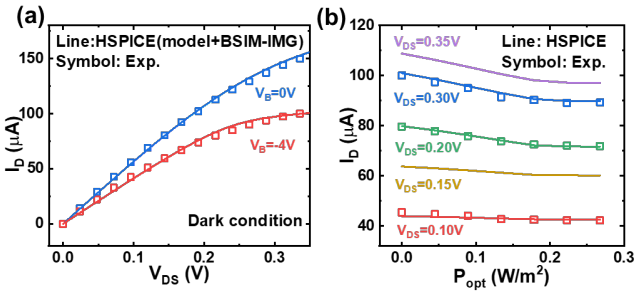


**Fig.6 a)** The dark $I_D$ obtained from HSPICE (based on model combined with BSIM-IMG) agrees well with the experiment. **b)** The $I_D$ related to $P_{opt}$ obtained by the HSPICE shows good agreement with experiment.

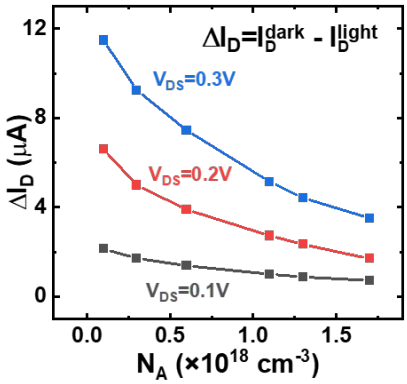


**Fig.7** The device light-induced $\Delta I_D$ related to the $N_A$ predicted from the model.

## III. ISC Evaluation

Using the model combined with BSIM-IMG, the array-scale ISC performance affected by the device design size and process variation can be evaluated. The $N_A$ variation is taken as evaluated example in this paper. As shown in Fig.7, predicted from our model, with higher $N_A$, the $I_D$ difference between dark and light condition ($\Delta I_D$) is decreased. Note that the $I_{ph}$ keeps almost constant with $N_A$ varying around $1\times10^{18}$ because $W_{dep} << \alpha$ and $\alpha^2 L_n^2 >> 1$ in the Eq.2 and Eq.3. The reason for the decreased $\Delta I_D$ is that the $\varphi_{BS}$ decreased more with the increasing $N_A$ according to the Eq.10 with the almost unchanged $Q_{BS}$.

Based on the effect of $N_A$ variation to the photoresponse of the pixel cell, the effect of $N_A$ variation to the in-sensor VMM is evaluated. As shown in Fig.8, the strategy of the VMM realized by the sensor array for evaluation is similar to

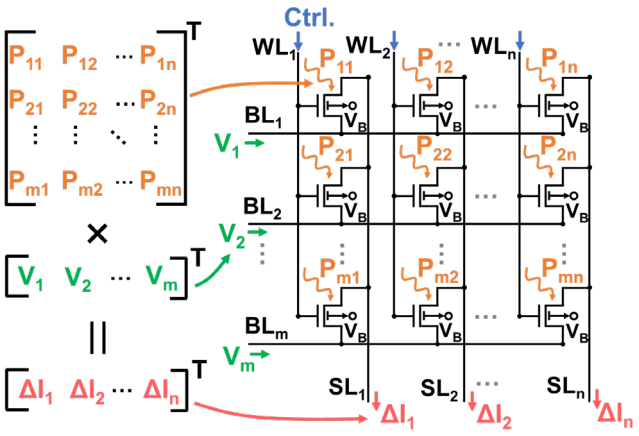


**Fig.8** The strategy schematic of the in-sensor VMM using the FDSOI based 1-T pixel sensor array.

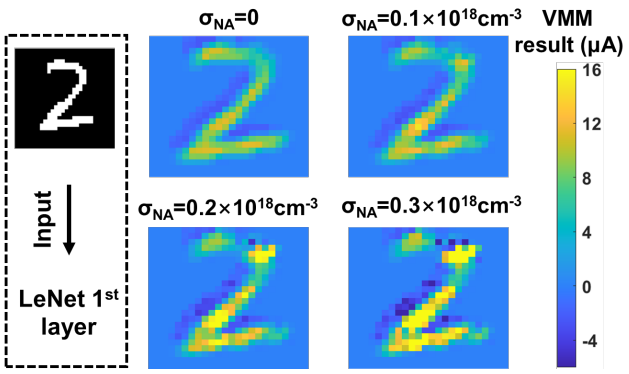


**Fig.9** The results of an example in-sensor VMM realized by device array with different $N_A$ variations. These results are simulated by HSPICE using the model combined with BSIM-IMG. The mean value of $N_A$ variation is set as $1.1\times10^{18}$ cm$^{-3}$.

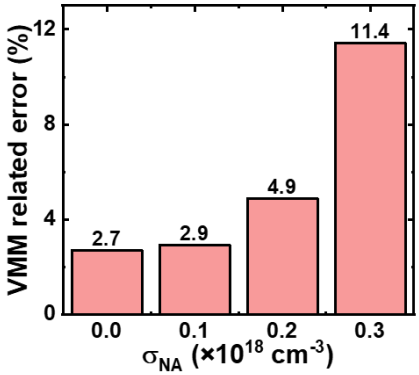


**Fig.10** The related error of the VMM with $N_A$ variations compared to the ideal result. With larger $N_A$ variation, the calculation error of VMM is enlarged. The error without variation mainly results from the non-linear $\Delta I_D$ response to $V_{DS}$.

our previous work [5]. The pixels are wired in the crossbar-like array. The signal applied on the WL is the enabling signal of the VMM operation. The input matrix is mapped as the light intensities of the input image. The vector is mapped to the $V_{DS}$ on the BLs. The operation results are obtained as the $\Delta I_D$s on the SLs. The positive vector elements and the negative elements are applied in the two different periods and their results are subtracted outside the array. The evaluated VMM results with different standard deviation of $N_A$ ($\sigma_{NA}$) are shown in the Fig.9. It shows that the larger/smaller result tends to be even larger/smaller with larger $\sigma_{NA}$. The reason is that smaller $N_A$ tends to occur with larger $\sigma_{NA}$, whose $\Delta I_D$ becomes larger according to the Fig.7. As shown in Fig.10, with the widened range of the results obtained from the pixel array with larger $\sigma_{NA}$, the related error to ideal is increased.

## IV. Conclusion

A compact model for photoresponse of FDSOI based 1-T pixel sensor is proposed for ISC and verified by both TCAD and experiment. By adding into BSIM-IMG, the photoresponse $I_D$ is obtained and the array-scale in-sensor VMM affected by $N_A$ variation is evaluated. The proposed model can help for the design of ISC applications based on FDSOI 1-T pixel sensor.


## Acknowledgment

This work was supported by the NSFC (62022006, 92064001, 62104007) and the 111 Project (B18001).

## REFERENCES


[1] L. Mennel, J. Symonowicz, S. Wachter, D. K. Polyushkin, A. J. Molina-Mendoza, and T. Mueller, "Ultrafast machine vision with 2D material neural network image sensors," *Nature,* vol. 579, no. 7797, pp. 62-66, 2020-03-05 2020, doi: 10.1038/s41586-020-2038-x.

[2] F. Liao, Z. Zhou, B. J. Kim, J. Chen, J. Wang, T. Wan, Y. Zhou, A. T. Hoang, C. Wang, J. Kang, J.-H. Ahn, and Y. Chai, "Bioinspired in-sensor visual adaptation for accurate perception," *Nature Electronics,* vol. 5, no. 2, pp. 84-91, 2022-02-01 2022, doi: 10.1038/s41928-022-00713-1.

[3] Z. Zhang, S. Wang, C. Liu, R. Xie, W. Hu, and P. Zhou, "All-in-one two-dimensional retinomorphic hardware device for motion detection and recognition," *Nat. Nanotechnol.,* vol. 17, no. 1, pp. 27-32, 2022-01-01 2022, doi: 10.1038/s41565-021-01003-1.

[4] B. Cui, Z. Fan, W. Li, Y. Chen, S. Dong, Z. Tan, S. Cheng, B. Tian, R. Tao, G. Tian, D. Chen, Z. Hou, M. Qin, M. Zeng, X. Lu, G. Zhou, X. Gao, and J.-M. Liu, "Ferroelectric photosensor network: an advanced hardware solution to real-time machine vision," *Nature Communications,* vol. 13, no. 1, 2022-12-01 2022, doi: 10.1038/s41467-022-29364-8.

[5] G. Yu, Z. Zhou, R. Chen, J. Li, P. Huang, J. Kang, and X. Liu, "Fully-Depleted Silicon-on-Insulator (FDSOI) Based Complementary Phototransistors for In-Sensor Vector-Matrix Multiplication," *IEEE Electron Device Lett.,* vol. 44, no. 4, pp. 670-673, 2023-04-01 2023, doi: 10.1109/led.2023.3248076.

[6] Y.-F. Cao, M. Arsalan, J. Liu, Y.-L. Jiang, and J. Wan, "A Novel One-Transistor Active Pixel Sensor With In-Situ Photoelectron Sensing in 22 nm FD-SOI Technology," *IEEE Electron Device Lett.,* vol. 40, no. 5, pp. 738-741, 2019-05-01 2019, doi: 10.1109/led.2019.2908632.

[7] S. Khandelwal, Y. S. Chauhan, D. D. Lu, S. Venugopalan, M. Ahosan Ul Karim, A. B. Sachid, B.-Y. Nguyen, O. Rozeau, O. Faynot, A. M. Niknejad, and C. C. Hu, "BSIM-IMG: A Compact Model for Ultrathin-Body SOI MOSFETs With Back-Gate Control," *IEEE Trans. Electron Devices,* vol. 59, no. 8, pp. 2019-2026, 2012-08-01 2012, doi: 10.1109/ted.2012.2198065.

[8] D. D. Lu, M. V. Dunga, C.-H. Lin, A. M. Niknejad, and C. Hu, "A computationally efficient compact model for fully-depleted SOI MOSFETs with independently-controlled front- and back-gates," *Solid·State Electron.,* vol. 62, no. 1, pp. 31-39, 2011-08-01 2011, doi: 10.1016/j.sse.2010.12.015.

[9] W. Chen, L. Cai, X. Liu, and G. Du, "Analytical Model for Interface Traps-Dependent Back Bias Capability and Variability in Ultrathin Body and Box FDSOI MOSFETs," *IEEE Trans. Electron Devices,* vol. 67, no. 11, pp. 4573-4577, 2020-11-01 2020, doi: 10.1109/ted.2020.3025979.

[10] S. M. Sze and K. K. Ng, *Physics of Semiconductor Devices*. New York: John Wiley & Sons, Inc., 2006.

[11] A. J. Scholten, G. D. J. Smit, R. Van Langevelde, and D. B. M. Klaassen, "The JUNCAP2 Model for Junction Diodes," in *Compact Modeling*: Springer Netherlands, 2010, pp. 299-326.